Optics Letters

Stimulated Raman scattering microscopy and spectroscopy with a rapid scanning optical delay line

Ruoyu He,[1] Zhiping Liu,[1] Yongkui Xu,[1] Wei Huang,[2,3] Hong Ma,[2,3] and Minbiao Ji[1,3,*]

[1]State Key Laboratory of Surface Physics and Department of Physics, Fudan University, Shanghai 200433, China
[2]State Key Laboratory of Genetic Engineering, Institute of Plant Biology, Department of Biochemistry and Molecular Biology, School of Life Sciences, Fudan University, Shanghai 200438, China
[3]Collaborative Innovation Center of Genetics and Development, School of Life Sciences, Fudan University, Shanghai 200433, China
*Corresponding author: minbiaoj@fudan.edu.cn

Received 18 November 2016; revised 4 January 2017; accepted 16 January 2017; posted 18 January 2017 (Doc. ID 280814); published 3 February 2017

Stimulated Raman scattering (SRS) microscopy that is capable of both high-speed imaging and rapid spectroscopy will be advantageous for detailed chemical analysis of heterogeneous biological specimens. We have developed a system based on spectral focusing SRS technology with the integration of a rapid scanning optical delay line, which allows continuous tuning of SRS spectra by scanning a galvo mirror. We demonstrate SRS spectral measurements of dimethyl sulfoxide solution at low concentrations and multi-color imaging of rice pollens and HeLa cells with line-by-line delay tuning to reduce motion artifacts, as well as fast acquisition of SRS spectra at specific regions of interest.

OCIS codes: (220.4830) Systems design; (170.0110) Imaging systems; (290.5910) Scattering, stimulated Raman; (170.5660) Raman spectroscopy.

https://doi.org/10.1364/OL.42.000659

Stimulated Raman scattering (SRS) microscopy has demonstrated unique chemical imaging capability and broad biomedical applications including label-free DNA imaging, drug delivery, tumor detection, lipid quantification, and bioorthogonal imaging [1–8]. One particular advantage of SRS over coherent anti-Stokes Raman scattering (CARS) is its undistorted spectra that replicate corresponding spontaneous Raman spectra [9], yet could be acquired much faster due to the coherent signal amplification [10]. Although it is the dream of researchers in the field to achieve both higher sensitivity (speed) and richer spectral information, in practice one still has to balance between them, and the various ways to compromise between sensitivity and spectroscopy of SRS have yielded technologies that target for different applications.

The highest sensitivity is achieved using picosecond narrowband lasers [3,4], which focus all the signal intensities onto one single Raman band. Thus, it can reach the highest imaging rate but suffers from sequential wavelength tuning in both multi-color imaging and spectral acquisition. These wavelength-sweeping-based methods include mechanical [1,3,11] and electro-optical [12,13] means, tuning wavelengths at different speeds either frame by frame or line by line. On the other hand, parallel spectral imaging could be realized using synchronized narrowband and broadband laser beams, with either dispersive detection [14–16] or excitation modulation multiplexing [17,18]. The former is spectrometer-based but requires array detectors and demodulators, which could be a few lock-in amplifiers [15], array LC resonators for more channels [16], or even array CMOS detectors [19], and they are largely limited to imaging thin specimens where tissue scattering is less of an issue. The latter modulates the wavelengths within the broadband at different RF frequencies, and SRS spectra could be retrieved with Fourier analysis. One can also use femtosecond broadband lasers for both pump and Stokes to achieve SRS/CARS spectra, including the implementation of Fourier transformation (FT) with delay scanning [20,21] or frequency comb [22], and the "spectral focusing" method with pulse-chirping [23–26]. FT SRS can achieve high-quality spectra but lacks the option of fast imaging. The spectral-focusing method tunes the SRS spectra by adjusting the optical delay line (ODL), and can achieve fast SRS imaging at chosen Raman bands as well as acquire SRS spectra by scanning the ODL, although conventional mechanical translational-stage-based ODL lacks the speed for fast spectroscopy.

In many cases, useful biomedical information lies in both the spatial mapping of biological tissues and the fine spectral analysis of particular regions of interests (ROI) [10]. Previous methods with single-color SRS imaging followed by spontaneous Raman spectral measurements of ROI have shown success in biochemical studies [27]. In this Letter, we develop a method of both rapid SRS imaging and spectroscopy by incorporating a rapid scanning optical delay line (RSODL) [28,29] into a spectral-focusing SRS system.

The experimental setup is illustrated in Fig. 1; it is based on a conventional spectral focusing apparatus where a femtosecond

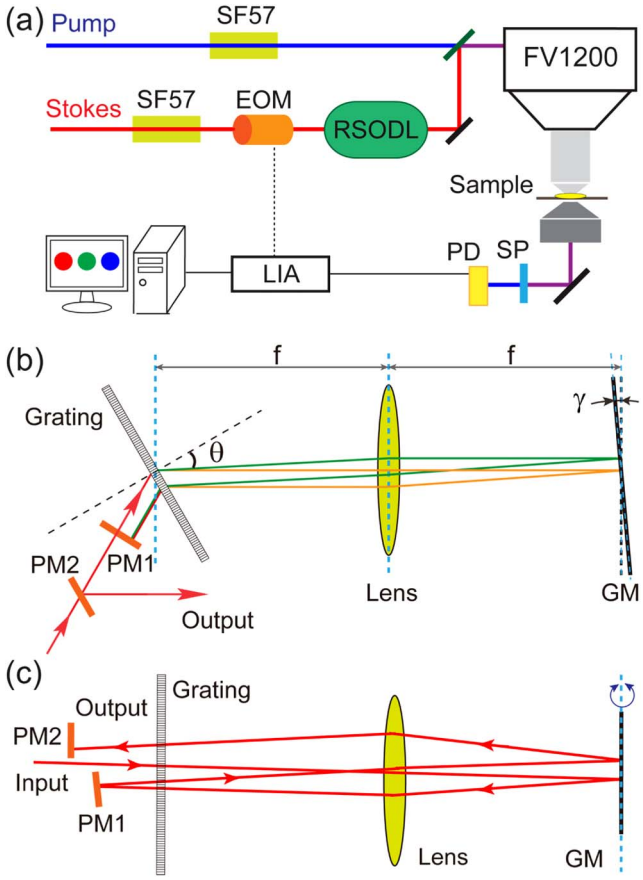

Fig. 1. Optical setup. (a) Illustration of spectral focusing SRS microscopy with a rapid scanning optical delay line (RSODL). (b) Top view and (c) side view of the RSODL. PM, pick-off mirror; GM, galvo mirror; PD, photo-diode; EOM, electro-optical modulator; LIA, lock-in amplifier; SP, short-pass optical filter.

pump and Stokes pulses were chirped by long glass rods (NSF57) to 3.8 and 1.8 ps, respectively. A RSODL was used to replace the translational stage so that the rotational angle could be converted into optical group delay [Fig. 1(a)]. The RSODL was composed of a grating, lens, and galvo mirror (GM) in a 4-f geometry [30,31], and was previously used in optical coherence tomography [30–32]. We further implemented two pick-off mirrors to double the beam path and, more importantly, to descan the output beam direction. The detailed layout of RSODL was illustrated in Figs. 1(b) and 1(c). The RSODL works effectively as a pulse shaper with the induced optical phase $\Delta\phi(\omega)$ and the optical group delay $\tau = \partial\Delta\phi/\partial\omega$. Theoretical deductions could be found in reference [28], and the optical delay is expressed as

$$\tau = \frac{\pi f p \lambda}{45c \cdot \cos\theta} \cdot \gamma, \tag{1}$$

where f is the focal length (100 mm) of the lens, λ is the center wavelength of the Stokes beam (1040 nm), γ is the rotation angle of the galvo (deg), c is the speed of light, p is the grating constant (1000 lines/mm), and θ is the diffraction angle (31°) of the transmission grating (LSFSG-1000-3212-94, LightSmyth). Because of much reduced inertia, RSODL could sweep the group delay in a much higher frequency than conventional

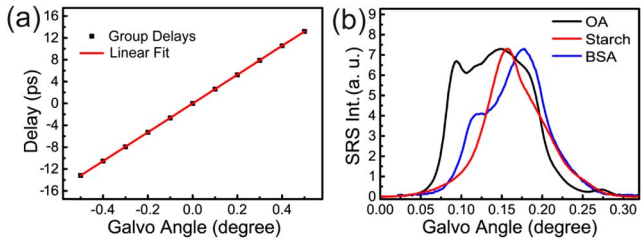

Fig. 2. Characterization of the RSODL. (a) Measured optical group delays at various rotation angles of the galvo mirror. (b) SRS spectra of standard test chemicals collected with the RSODL.

translational stage. As a proof-of-principle work, we were using a galvo mirror (GVS001, Thorlabs) that could work up to 1 kHz for small angle rotations (–0.2°).

A standard high-frequency modulation-transfer scheme was used to detect the SRS signal [4,12]. Pulsed femtosecond beams from a commercial optical parametric oscillator (OPO) laser (Insight Deepsee, Newport, California, U.S.) served as the laser source. The tunable OPO output acted as the pump beam and the 1040 nm beam was used as the Stokes beam, whose amplitude was modulated at 20 MHz. The spatially and temporally overlapped pump and Stokes beams were sent through a laser-scanning microscope (BX61WI/FV1200, Olympus) and focused onto the sample. The SRS signal was demodulated with a commercial lock-in amplifier (HF2LI, Zurich Instrument). The microscope provided triggering TTL outputs of pixel, line, and frame events, which could be used to synchronize with the RSODL to work under frame or line mode for SRS spectral imaging. In this Letter, we mainly use line mode to achieve multi-color SRS.

We first characterized the performance of the RSODL by measuring the amount of delay τ as a function of galvo rotation angle γ. The delay was measured by a translational stage in the setup with cross-correlation measurements, and the rotation angle was converted from the voltage applied to the galvo. Experimental data is shown in Fig. 2(a), with a perfect linear fit of 26.36 ps/deg. Our measured slope agrees with the theoretical value from Eq. (1) (28.23 ps/deg) quite well.

We validated the system by collecting SRS spectra of standard test chemicals: oleic acid, starch, and bovine serum albumin. As can be seen in Fig. 2(b), all the acquired RSODL-SRS spectra agreed with previous results using translational-stage-based ODL [33]. We estimated a correlation of 805 cm^{-1}/deg between the Raman shift and the galvo angle. Within a spectral range of 200 cm^{-1}, the GM only needs to rotate ~0.3°, as shown in Fig. 3(a). Under this small angle condition, the GM could work at 1 kHz, which enabled us to take 2000 spectra in 1 s when the GM was driven by symmetrical triangular waveform. Therefore, each spectrum cost 500 μs, composed of 250 data points (2 μs/point). After averaging, the signal to noise ratio (SNR) and detection sensitivity could be significantly improved. We took SRS spectra of dimethyl sulfoxide (DMSO) at different concentrations by targeting the 2909 cm^{-1} Raman band, which could be clearly identified down to the concentration of 1 mM with 10 s acquisition time [Fig. 3(b)]. All spectra were corrected by removing the background envelopes that might be originated from water contribution, especially at low DMSO concentrations. We also

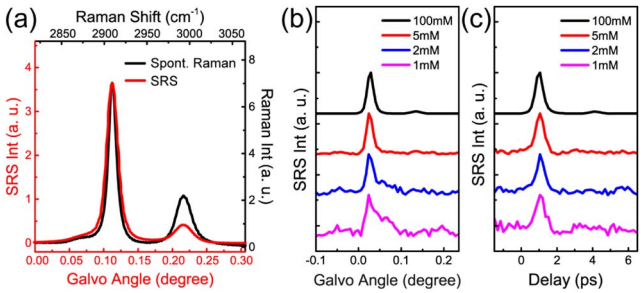

Fig. 3. SRS spectral measurements. (a) Spontaneous and stimulated Raman spectra of DMSO. (b) SRS spectra of DMSO aqueous solutions with RSODL (1 kHz scanning rate, 10 s averaging). (c) SRS spectra of DMSO solutions with translational stage (1 s per data point, 60 data points).

compared the spectra with that from translational-stage-based ODL [Fig. 3(c)] and showed similar sensitivity between them.

Our system is also ideal for multi-color SRS imaging with line-by-line spectral tuning, as previously demonstrated with electro-optical tunable OPO [12]. To do that, a FV1200 microscope was operated in the "Line Kalman" mode, where each line scans multiple times before moving to the next. A line trigger signal from the FV1200 analog interface box was utilized to synchronize with the driving voltages (step functions) for the RSODL by a data-acquisition card (USB-6363, National Instruments), so that each line within the Kalman period was at a different optical delay. The delay was switched at the falling edge of the line trigger to ensure enough time for the delay GM to settle (~300 μs) during the flyback (1 ms) of the imaging GMs. Recorded raw SRS signal using the same data acquisition card was reconstructed to form multiple images, each of which corresponded to a preset Raman frequency. Subsequent numerical decomposition algorithms were applied to extract the images of multiple chemical components.

We demonstrated the line mode multi-color imaging ability by chemical mapping of plant and mammalian cells. Figure 4(a) shows a three-color SRS image of two rice pollen grains at different development stages [34,35]. Images were taken at 512 × 512, 2 μs/pixel, and Kalman mode of three lines to image at three optical delays as marked in Fig. 4(b). Three-color images representing lipid, protein, and starch distributions were reconstructed by linear decomposition algorithm [1,17]. The left small pollen belonged to an early stage and mainly contained lipids (red) and proteins (blue), while the right big one was relatively mature and full of starch (green). Such a multi-color SRS technique allows for quantitative biochemical studies of rice pollens during the developmental process. In addition, SRS spectra from different ROI could be conveniently acquired at high speed. For instance, we could zoom in and park the laser spot onto different locations to rapidly measure their spectra [Figs. 4(a) and 4(b)]. As expected, the SRS spectra from regions 1–3 correspond to that of lipids, proteins, and starches. Each spectrum was taken in 200 ms with high SNR, indicating the potential of our method for fast spectral analysis on different ROI.

We also imaged live HeLa cells to demonstrate the capability of our method to reduce motion artifacts caused by the drift of live organelles during the imaging process [12]. While significant motion artifacts were seen from the frame-by-frame

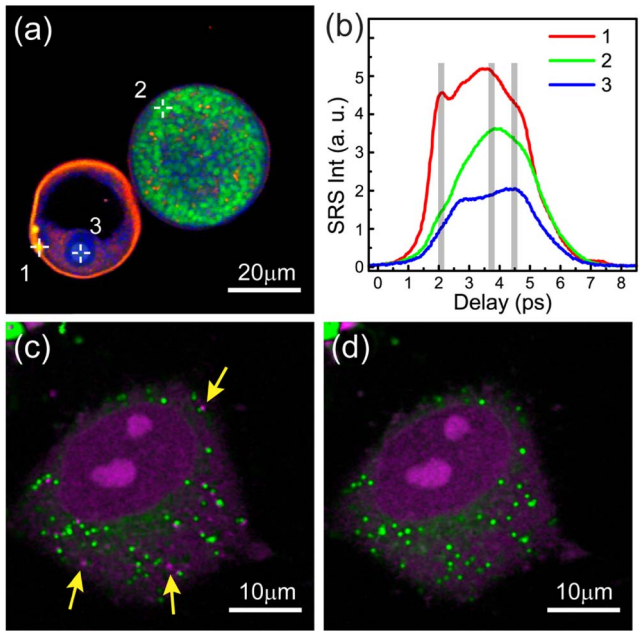

Fig. 4. SRS imaging and spectroscopy of biological samples. (a) Three-color image of rice pollen grains acquired with line-by-line spectral tuning mode. Lipids, starches, and proteins are false-colored red, green, and blue, respectively. (b) SRS spectra of three ROIs marked 1, 2, and 3 in (a), each acquired with 200 ms. (c) Frame-by-frame and (d) line-by-line images of live HeLa cell, showing lipid (green) and protein (magenta) distributions; motion artifacts caused by drifting lipid droplets are shown with arrows.

method [Fig. 4(c)], little artifacts could be detected with the line-by-line mode [Fig. 4(d)]. Since each line consumes 1 ms, such a method is able to reduce artifacts caused by motions slower than the millisecond time scale. For faster-moving objects such as flowing cells, parallel imaging methods are preferred.

The method presented in this Letter has several advantages over previous ones. Compared with the method using electro-optical tunable OPO [12], which has inevitable settling time (tens of microseconds) for the OPO laser when adjusting the wavelengths, our method can reach a faster spectral tuning rate, as fast as the galvo mirror could operate. Compared with the parallel detection scheme with excitation multiplexing [15,16], our method can acquire more continuous spectra without sacrificing the sensitivity. For multi-color imaging, we can achieve 16-channel SRS images simply by increasing the Kalman number to 16 with the total imaging time of ~16 s, while the previous method took ~30 s [16]. But increasing the Kalman number has the drawback of more motion artifacts, since each spectrum effectively costs 16 ms versus 60 μs in the previous method [16].

To compare detection sensitivity, we noticed that Figs. 3(b) and 3(c) showed similar SNR but that less acquisition time was used for the RSODL-based method [Fig. 3(b)]. At low concentrations, the sensitivity is largely limited by solvent background either from residual Raman contribution or cross-phase modulation, which overwhelm the analyte signal. If the laser intensity has low-frequency fluctuations, it will cause background fluctuations which will reduce detection sensitivity in the slow sequential point-by-point spectral measurements as in Fig. 3(c).

Under such circumstances, parallel detection methods and rapid sweeping methods could help increasing SNR by averaging out common mode noise.

In conclusion, we have combined a rapid scanning optical delay line with spectral focusing SRS to achieve both high-speed imaging and spectral acquisition. By scanning the angle of the GM in the RSODL, continuous optical delay is rapidly and conveniently produced. SRS spectra could be collected within 500 μs and, by reducing low-frequency laser noise, the spectral SNR and sensitivity could be improved. Our method provides the flexibility to either perform high-speed multi-color SRS imaging without motion artifacts or rapid spectral measurements on particular regions of interest to assist more detailed chemical analysis.

Funding. National Natural Science Foundation of China (NSFC) (81671725); Shanghai Rising Star Program (15QA1400500); Shanghai Action Plan for Scientific and Technological Innovation Program (16441909200); National Key Research and Development Program of China (2016YFA0301000, 2016YFC0102100).

REFERENCES

1. F.-K. Lu, S. Basu, V. Igras, M. P. Hoang, M. Ji, D. Fu, G. R. Holtom, V. A. Neel, C. W. Freudiger, and D. E. Fisher, Proc. Natl. Acad. Sci. USA **112**, 11624 (2015).
2. B. G. Saar, L. R. Contreras-Rojas, X. S. Xie, and R. H. Guy, Mol. Pharm. **8**, 969 (2011).
3. B. G. Saar, C. W. Freudiger, J. Reichman, C. M. Stanley, G. R. Holtom, and X. S. Xie, Science **330**, 1368 (2010).
4. C. W. Freudiger, W. Min, B. G. Saar, S. Lu, G. R. Holtom, C. He, J. C. Tsai, J. X. Kang, and X. S. Xie, Science **322**, 1857 (2008).
5. M. Ji, S. Lewis, S. Camelo-Piragua, S. H. Ramkissoon, S. M. S. Venneti, A. Fisher-Hubbard, M. Garrard, D. Fu, A. C. Wang, J. A. Heth, C. O. Maher, N. Sanai, T. D. Johnson, C. W. Freudiger, O. Sagher, X. S. Xie, and D. A. Orringer, Sci. Trans. Med. **7**, 309ra163 (2015).
6. M. Ji, D. A. Orringer, C. W. Freudiger, S. Ramkissoon, X. Liu, D. Lau, A. J. Golby, I. Norton, M. Hayashi, N. Y. Agar, G. S. Young, C. Spino, S. Santagata, S. Camelo-Piragua, K. L. Ligon, O. Sagher, and X. S. Xie, Sci. Transl. Med. **5**, 201 (2013).
7. C. Cao, D. Zhou, T. Chen, A. M. Streets, and Y. Huang, Anal. Chem. **88**, 4931 (2016).
8. L. Wei, F. Hu, Z. Chen, Y. Shen, L. Zhang, and W. Min, Acc. Chem. Res. **49**, 1494 (2016).
9. K. A. Antonio and Z. D. Schultz, Anal. Chem. **86**, 30 (2014).
10. J. X. Cheng and X. S. Xie, Science **350**, aaa8870 (2015).
11. M. C. Wang, W. Min, C. W. Freudiger, G. Ruvkun, and X. S. Xie, Nat. Methods **8**, 135 (2011).
12. L. Kong, M. Ji, G. R. Holtom, F. Dan, C. W. Freudiger, and X. X. Sunney, Opt. Lett. **38**, 145 (2013).
13. S. Karpf, M. Eibl, W. Wieser, T. Klein, and R. Huber, Nat. Commun. **6**, 6784 (2015).
14. L. Czerwinski, J. Nixdorf, G. D. Florio, and P. Gilch, Opt. Lett. **41**, 3021 (2016).
15. F. Lu, M. Ji, D. Fu, X. Ni, C. W. Freudiger, G. Holtom, and X. S. Xie, Mol. Phys. **110**, 1927 (2012).
16. C. Liao, M. N. Slipchenko, P. Wang, J. Li, S. Y. Lee, R. A. Oglesbee, and J. Cheng, Light Sci. Appl. **4**, e265 (2015).
17. F. Dan, F. K. Lu, Z. Xu, C. Freudiger, D. R. Pernik, G. Holtom, and X. S. Xie, J. Am. Chem. Soc. **134**, 3623 (2012).
18. C. Liao, P. Wang, P. Wang, J. Li, H. J. Lee, G. Eakins, and J. Cheng, Sci. Adv. **1**, e1500738 (2015).
19. W. Rock, M. Bonn, and S. H. Parekh, Opt. Express **21**, 15113 (2013).
20. J. Réhault, F. Crisafi, V. Kumar, G. Ciardi, M. Marangoni, G. Cerullo, and D. Polli, Opt. Express **23**, 25235 (2015).
21. K. Hashimoto, M. Takahashi, T. Ideguchi, and K. Goda, Sci. Rep. **6**, 21036 (2016).
22. T. Ideguchi, S. Holzner, B. Bernhardt, G. Guelachvili, N. Picqué, and T. W. Hänsch, Nature **502**, 355 (2013).
23. D. Fu, G. Holtom, C. Freudiger, X. Zhang, and X. S. Xie, J. Phys. Chem. B **117**, 4634 (2013).
24. D. Fu, Y. Yu, A. Folick, E. Currie, R. V. Farese, Jr., T. H. Tsai, X. S. Xie, and M. C. Wang, J. Am. Chem. Soc. **136**, 8820 (2014).
25. D. Fu, J. Zhou, W. S. Zhu, P. W. Manley, Y. K. Wang, T. Hood, A. Wylie, and X. S. Xie, Nat. Chem. **6**, 614 (2014).
26. S. Funkner, K. Saito, G. Niehues, Y. Yazawa, T. Furuya, K. Yamamoto, and M. Tani, Appl. Phys. Lett. **105**, 021103 (2014).
27. M. N. Slipchenko, T. T. Le, H. Chen, and J. X. Cheng, J. Phys. Chem. B **113**, 7681 (2009).
28. G. J. Tearney, B. E. Bouma, and J. G. Fujimoto, Opt. Lett. **22**, 1811 (1997).
29. K. F. Kwong, D. Yankelevich, K. C. Chu, J. P. Heritage, and A. Dienes, Opt. Lett. **18**, 558 (1993).
30. K. K. M. Silva, A. V. Zvyagin, and D. D. Sampson, Electron Lett. **35**, 1404 (1999).
31. A. Rollins, S. Yazdanfar, M. Kulkarni, R. Ung-Arunyawee, and J. Izatt, Opt. Express **3**, 219 (1998).
32. G. J. Tearney, M. E. Brezinski, B. E. Bouma, S. A. Boppart, C. Pitris, J. F. Southern, and J. G. Fujimoto, Science **276**, 2037 (1997).
33. R. He, Y. Xu, L. Zhang, S. Ma, X. Wang, D. Ye, and M. Ji, Optica **4**, 44 (2017).
34. T. Kerim, N. Imin, J. J. Weinman, and B. G. Rolfe, Proteomics **3**, 738 (2003).
35. V. Raghavan, Am. J. Bot. **75**, 183 (1988).